OFDM aplied to Free Space Optics

line 1: João Salgueiro
line 2: *Instituto de Telecomunicações*
line 3: *Instituto Superior Técnico*
line 4: Lisboa
line 5: joao.salgueiro@ist.utl.pt

This dissertation takes as central axis the proof of concept of a free space optical transmission through the implementation of OFDM for the coding of the signal. Is introduced a brief historical context of the optical communications, and the state of art related to the currently used Free Space Optics technologies is presented, also a description of them is made based on the transmission distance. Following are the fundamental theoretical concepts inherent to any optical communications system, paying attention to the types of optical source, optical receiver and lens. Several modulations commonly used in these systems are described, such as OOK modulation, among others. The use of OFDM modulation is proposed, and the different aspects of the OFDM modulation are then analyzed. A brief description is also given of the various types of atmospheric attenuation and their effects on a Free Space Optics system, as well as the Rayleigh multipath and dispersion concept. It is also presented the method used in the evaluation of this type of systems. In the accomplishment of the dissertation a computer simulation component was implemented to simulate the transmission channel, in which the impacts of the guard interval for the different sub modulations were studied. Finally, the experimental implementation was performed for three attenuation values and the best sub modulation to be used for each case was studied, taking into account the limitations of binary errors imposed for signal transmission.

I. Introduction

Wireless technologies are one of the great success stories in the history of technology, fulfilling the dream of humans to communicate from anywhere at any time. Although voice communication has been the main service for 15 years, mobile data and wireless Internet have become widespread much faster than anyone could have imagined. Nowadays, the term "wireless" is widely used as a synonym for radio frequency (RF) technologies as a result of its worldwide market dominance. The RF band is between 30 kHz and 300 GHz of the electromagnetic spectrum and its use is strictly regulated by local and international authorities. In most cases, the sub-bands are licensed exclusively to operators, such as telephone operators, television broadcasters, point-to-point microwave links, among others [1]. The exponential increase of commercial demand for high-speed wireless broadband was an attempt to accommodate the increasing use of internet and multimedia services among mobile users, residential and business clusters. This has stimulated an extraordinary growth in data traffic in the last decade, growing at a rate that exceeds the prediction of Moore's law [2]. As a result, data traffic has increased exponentially, corresponding to a growth in global traffic volume of hundreds of times in the next decade [3].

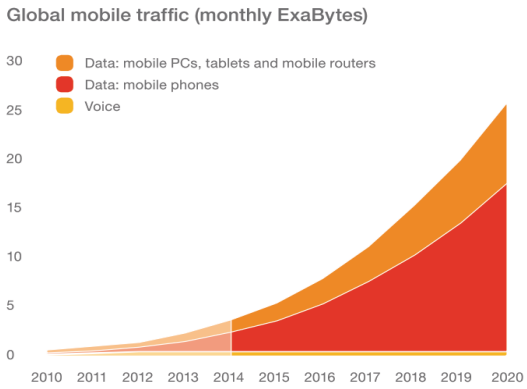

Fig. 1. Global mobile traffic measured monthly in ExaBytes [2].

There are two options available to solve this problem, the first is to better optimize RF-based technologies, however, regardless of the technologies (3G, 4G, 5G or Wi-Fi) adopted, there are three approaches to increase the capacity of wireless radio. The first is the launch of a new spectrum and therefore more bandwidth, the second is the creation of more nodes and the third is elimination of interference. Acquiring a new spectrum is very expensive. Finding more bandwidth is not a big problem, but clearly it is not enough because even this is finite. Additional nodes can be included through cell division, which is quite expensive. In addition, two nodes do not offer double the capacity of one, due to interference problems [4].

Another technology that allows addressing and overcoming these restrictions is free space optical communication or Free Space Optics (FSO). Unlike common RF systems operating in a frequency range between 2.4 GHz and 5.7 GHz with transfer rates ranging from 2 Mbps to 400 Mbps, FSO technology has data transfer rates exceeding 2.5 Gbps and using a wide unlicensed spectrum range between 700 nm and 10000 nm, offering virtually unlimited bandwidth. This technology includes infrared, visible and ultraviolet [5].

II. State of Art

FSO technology can potentially be used in a wide range of communication applications [3]. These applications can range from optical connections within integrated circuits, terrestrial links or even satellite communications. The applications of FSO communications can be divided by reaches, passing these by ultra-short, short, medium, long and ultralong. Ultra-short-range applications arise to accommodate the increasing demands of exascale computing and data centres. Unconventional methods for inter-chip and intra-chip communications have been explored [4]. With superior characteristics such as high bandwidth and low latency, optical interconnections were proposed as an alternative to copper-based electrical connections that became a major bottleneck in the design of these systems [6].

Optical interconnections can be implemented with waveguide or in free space. In guided optical interconnections, loss in the waveguide, cross section and minimum radius of

curvature dominate the design process. Optical connections in free space provide a more flexible solution and can achieve a high degree of parallelism. In a study conducted by CIR in 2014, the market for optical chip interconnections will reach almost 520 million dollars by 2019, reaching 1020 million dollars by 2021.

We can consider that we leave the ultrashort range and enter the short range when the transmission distance changes to the order of ten centimeters. A common short-range application is the Wireless Area Body Network (WBAN), which involves the use of wearable electronic devices or sensors for the transmission of the individual's physical and biochemical information. In a typical WBAN, there are several sensors placed in the human body that record vital signs like blood pressure, heart rate, glucose, among others. These sensors are wirelessly connected to a central unit that has access to an external network [4].

Current WBANs are generally supported by RF, but their use can be problematic in medical facilities and hospitals where RF installation is prohibited due to electromagnetic interference. Recent discoveries in the field of organic LEDs make it possible to integrate optical transmitters into garments as part of a WBAN. Some hospital test equipment such as a cardiac stress test can also be altered by integrating LEDs into the sensors and replacing the large number of cables required by visible spectrum optical connections.

Another example of a short-range application is the Wireless Personal Area Network (WPAN) that involves "last meter" connectivity to interconnected devices centered around a person's workspace. FSO technology in the form of infrared LED communication has been used effectively in WPANs since the mid-1990s. The Giga-IR standard developed by the Infrared Data Association allows the transmission of 1 Gbps. A new standard is still being developed that will allow it to raise speeds to 5 and up to 10 Gbps. Recent research efforts in this area include smartphone camera communications, where the phone's integrated camera is used as an optical detector to allow various machine-to-machine (M2M) applications, including telephone to phone, telephone to TV and telephone to automatic vending machine, among others.

When the transmission distance is in the order of meters, we are dealing with medium range applications. A possible medium-range application is the wireless local area network (WLANs). In the past, indoor infrared communication was widely investigated as a possible WLAN solution. However, the success of RF-based solutions such as WiFi has conditioned its implementation. However, this situation can easily change with the emergence of VLC, also known as LiFi. New generations of LEDs have attractive features such as long-life expectancy, high humidity tolerance, lower power consumption and lower heat dissipation. Incandescent lamps and fluorescent lights have gradually been replaced by energy-efficient lighting technologies, so LEDs are expected to be the main source of light soon [4].

VLC leverages the expected omnipresence of LED-based lighting infrastructure and enables a wireless network with high transmission rates, minimizing interference problems due to the spatial confinement of LEDs. A research done in 2013 showed that the spectral efficiency of the indoor area can be improved by a factor of 900 when using a VLC based WLAN [7]. In VLC experimental trials were reached the maximum transfer rates of 3 Gbps [8].

In addition to the interior installation, the LEDs are being used extensively in outdoor lighting, traffic lights, advertising screens, headlights and rear lights of automobiles, among others. This new development opens the way for vehicle-vehicle and vehicle-infrastructure communication. Vehicles equipped with LED-based front and rear lights can communicate with each other and with the infrastructure near the road, i.e. streetlights, traffic lights, among others, using VLC technology [9]. In addition, this system can still be used for both signalling and the transmission of information related to the safety of vehicles on the road. The VLC is well-positioned to address the low latency required in safety features such as electronic emergency braking lights, collision warning.

FSO systems can also be used for high-speed communication between two fixed points at several kilometres. In a study carried out in 2013 between the Aveiro telecommunications institute and the University of Rome, it was concluded that an FSO connection enjoys a very high optical bandwidth when compared to RF, allowing data transfer rates in the order of Tbps [10]. FSO systems initially attracted attention as an efficient solution to the "last mile" problem to bridge the gap between the end user and the fiber optic infrastructure already installed. FSO systems can also be used for a variety of long-range communications applications, including metropolitan area wireless (WMAN) extensions, WLAN connectivity for WLAN in corporate and institutional environments, and wireless broadband access to remote areas for the purposes of video surveillance [4].

Nowadays it is also possible to establish FSO links between mobile points, due to the new localization algorithms, thus allowing the implementation of FSO links between two aircraft, or between the aircraft and the base. This technology has considerable military interest [11].

FSO communications can even be used as a powerful ultralong link solution corresponding to distances greater than 10,000 kilometers for inter-satellite communications or satellite-to-terrestrial communications as well as interplanetary communication. One of the major milestones in this area occurred in 2001 when a 50 Mbps FSO link was established for the first time between two terrestrial satellites. The experience of the European Space Agency consisted of a satellite link using semiconductors and was successfully established between the ARTEMIS geostationary satellite and the SPOT-4 ground-based observation satellite [12]. These rates subsequently went on to the order of gigabits per second with the introduction of coherent modulation techniques. In October 2013, in a NASA laser communication demonstration, an FSO link was established between the Moon and Earth, where an impressive data rate of 622 Mbps was achieved on a 38,400-kilometer route. Proving that FSO communication is a technology with spatial applications and may even complement or replace the RF in this area [4].

III. THEORETICAL GROUNDING

Commercially available FSO systems use wavelengths close to the visible spectrum between 850 nm and 1550 nm, corresponding to frequencies in the order of 200 THz [13]. An FSO system consists of a transmitter that receives an electric signal, transforms it into an optical signal and sends it in beam form through the atmosphere. On the other side we have a receiver that receives this optical signal and converts it back into an electric signal.

The Emitter can be divided into 4 parts, encoder, modulator, optical source and lens. The encoder is responsible for encoding the electrical impulses to be transmitted, which can be adapted to the requirements of the application. The function of the modulator is the aggregation of multiple pulses and reconversion into another electrical signal that adapts to the current requirements of the optical source. The optical source can pass through a LED or a Laser capable of performing the electro-optical conversion and transmission of the modulated signal. Finally, we have the lens that allows the concatenation of the emission beam of the optical source, in order to increase the maximum amplitude of the signal power in the receiver, decreasing the divergence of the beam [14].

On the receiver side, we start with the lens that has the same effect as the emission system. It is followed by a photodetector, responsible for the electric opto-conversion, in which the optical signal is converted to a current proportional to its amplitude. Finally, the digital signal processor performs the analog to digital conversion of the signal, sending that information to the demodulator which translates it into electrical impulses. These signals are then converted into binary code and sent to a processing unit.

A. *System Implementation*

With access to DACs / ADCs with sampling rates of giga samples per second on transmitters that allow direct conversions from the analog to digital domains and vice versa becomes more attractive than the use of analog modulators. This concept greatly simplifies the system, maintaining all signal processing in the digital domain and eliminating the normal difficulties associated with analog components [15].

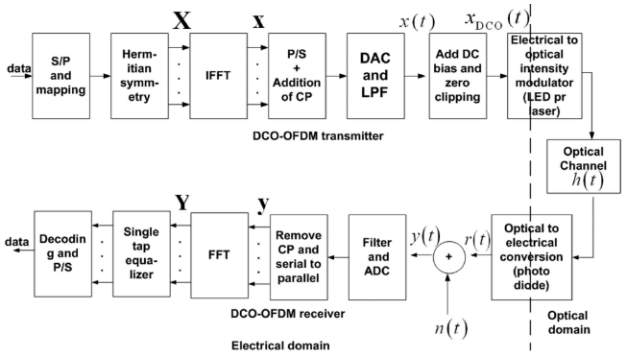

Fig. 2. Block diagram of an optical communication system using OFDM (adapted from [15]).

Figure 2 shows a block diagram of an optical communication system using OFDM. First, the high-bitrate serial data stream is divided into N parallel data streams of lower bitrate. Each data stream is then encoded into a complex value using amplitude and quadrature (QAM) or phase shift (PSK) modulation, further using Hermitian symmetry to convert the complex signal to real in the time domain. These complex values are then mapped to a vector, transmitted through the channel and the inverse process is made in the receiver end.

After dividing the original signal into N bands for the purpose of eliminating the ISI, a guard interval can be entered at the beginning of each OFDM symbol. The guard interval is greater than the maximum propagation delay on the channel. The orthogonality between subcarriers is preserved by keeping the period of the symbol equal to the observation period plus the guard interval in order to also prevent inter-carrier interference (ICI) [15]. The cyclic prefix is added as a guard interval. This prefix consists of a copy of the last part of the OFDM symbol that is added to the beginning of the symbol as a guard interval. In the case of an OFDM symbol consisting of N symbols with a period of observation, which in this case will be defined at the exit of the IFFT, the cyclic prefix consists of the last symbols of the original symbol as shown in Figure 24 and Figure 25. Typically, the number of samples contained in the cyclic prefix is represented by N_g.

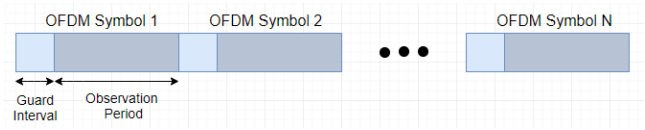

Fig. 3. OFDM symbols with guard interval

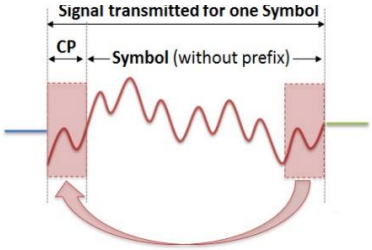

Fig. 4. Cyclic Prefix on an OFDM symbol.

Even after the addition of the cyclic prefix to the OFDM symbol the time samples are not suitable for transmission in the channel since the non-negativity of the samples has not yet been guaranteed [16]. This problem is usually solved by using a DC component that is added to the time samples. In the receiver, demodulation and decoding of the data is performed. The orthogonality of the subcarriers allows the receiver to be able to separate each carrier and perform the maximum likelihood detection QAM or PSK. The detected information is then compared to the transmitted signal and the binary error rate (BER) is used as a way of analyzing the performance of the system.

As previously mentioned, unlike non-optical OFDM systems in which the information is transmitted in the electric field and the signal may have positive or negative (bipolar) values, since in the receiver there is a local oscillator and coherent detection is used. In a typical intensity modulated direct detection optical system, the information is transmitted at the optical signal intensity and therefore can only be positive or unipolar. One method used to ensure non-negativity of the transmitted signal is to add a DC component to the OFDM signal. The DC component required to satisfy the condition of the signal to be positive is equal to the maximum negative amplitude of the OFDM signal [16].

For a large number of subcarriers, the amplitude of the OFDM signal can be approximated by a Gaussian distribution. For the random variable x with Gaussian distribution of mean zero and with standard deviation σ, the probability of the random variable being in the region of $-2\sigma < x < -2\sigma$ equals 95.6%. This results in,

$$Pr\{x + 2\sigma > 0\} \cong 97.8\%$$

Since this result is quite close to 1, in recent work it is suggested to add a DC component equal to twice the standard deviation of the bipolar OFDM signal and to cut the resulting amplitudes. This method requires a smaller DC component, however it suffers from the distortion caused by cutting noise.

Although this is the simplest compatibility scheme for IM / DD channels, it suffers from poor optical power efficiency.

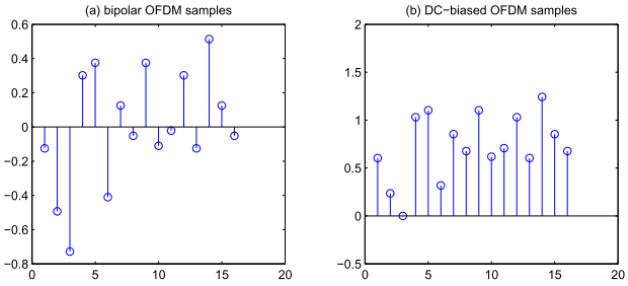

Fig. 5. Conversion of Bipolar OFDM to OFDM with DC component (adapted from [17]).

B. *Benefits*

OFDM modulation has several advantages, such as the high bitrate in the channel and the implementation using IFFT and FFT as a tool. OFDM also has good inter-symbol interference (ISI) tolerance. The advantages of OFDM are listed below:

- Easily adaptable to severe channel conditions without the need for complex equalizations.
- Rugged against narrowband co-channel interference.
- Robust against intersymbol interference (ISI) and fading caused by multipath propagation.
- High spectral efficiency.
- Efficient implementation using FFT.
- Low sensitivity to temporal synchronization errors.
- No sub-channel filters are required tuned to the receiver as opposed to FDM.

C. *Disadvantages*

On the other hand, this modulation has some disadvantages. The main disadvantage of OFDM is complexity. Being a multi-carrier modulation, it becomes more complex than a single carrier modulation. The disadvantages of OFDM are listed below:

- Sensitive to Doppler shift.
- Sensitive to frequency synchronization problems.
- High peak to average power ratio (PAPR).

IV. Computer Simulation

A. *Model*

In order to create a Matlab simulation of an optical system in free space, the following steps were performed:

A data matrix was created with random integers generated through a normal distribution, with values between 0 and the modulation index minus one. That is, if for example the modulation used to modulate the subcarrier is 4QAM, the modulation index will be 4 and the array values will be comprised between 0 and 3. Each row of the array represents a data subcarrier while the number of columns is determined by the size of the window or the amount of OFDM symbols to be observed. The matrix mapping was then performed using the QAM or PSK constellation.

In an OFDM system with N subcarriers the following condition is imposed:

$$C_{-k} = C_k^* \ , C_0 \in \mathbb{R}$$

Where C_k is the complex value of the subcarrier with index $k \in [-\frac{N}{2} \dots \frac{N}{2} - 1]$. This can be achieved by mapping complex $N/2$ symbols on subcarriers 0 through $N/2 - 1$ and assigning the remaining conjugate complexes to negative index subcarriers. Since the signal to be transmitted in the laser must be composed of real values and knowing that the DFT of a real signal has a Hermitian symmetry, it is easy to understand the importance of performing a Hermitian symmetry of the signal before performing the IDFT.

Then the zero padding is done which consists of creating an array where the number of rows is defined by the number of FFT points and the number of columns defined by the window size. The first half of the Hermitian symmetry matrix is then copied to the first positions of this new matrix and the second half to the end of this new matrix, thus leaving the new matrix with a range of lines with no values at its center. This method avoids errors related to convolution of the signal with the channel, since the linear convolution of two vectors is always greater than any of the vectors. This avoids the risk of extra convolution values being distributed throughout the matrix.

The modulation is then performed through the fast Fourier transform algorithm. Using a larger FFT allows you to index more points in the frequency which can result in a better defined spectrum. The next step is the introduction of the guard interval and concatenation of the data array into a vector which is subsequently normalized and converted to values that can be transmitted in the linear laser regime.

Then it is necessary to generate the time and frequency vectors. A time vector is created with the data vector dimension and spacing equal to the sampling period. Total time and bandwidth are also calculated. A vector of frequencies with positive frequencies is also created in the first part of the vector and the negative frequencies in the second part.

For the communication channel, the Rayleigh multipath channel model is considered. This can be modeled as an n-taps channel in which each real and imaginary part is an independent Gaussian random variable. These taps correspond to delays caused by the multipath. The impulse response can be expressed by:

$$h(t) = \frac{1}{\sqrt{n}}[h_1(t - t_1) + h_2(t - t_2) + \cdots + h_n(t - t_n)$$

Where $\frac{1}{\sqrt{n}}$ corresponds to the channel power normalization. The real and imaginary part of each tap has variance ½ and mean 0. Convolution of the signal transmitted with the channel is then carried out and the AWGN noise is inserted.

On the receiver side the first step is to remove the transformation that was made to the signal so as to be transmitted in the linear laser regime. The standardization is then withdrawn, the conversion is carried out from series to parallel and the guard interval is withdrawn. The next step

involves the demodulation of the signal at defined points and channel recognition. This recognition is done by dividing the received symbol matrix by the transmitted symbol matrix. The zero forcing is then performed which consists of applying the inverse frequency response of the channel to the received signal in order to restore the signal after the channel. Then the zero padding is removed and the Hermitian symmetry is undone. The final step in reception is the detection of received symbols through QAM or PSK demodulation. In order to be able to evaluate the transmission, the number of errors and the error rate per bit are calculated.

B. Results

A transmission model with 160 subcarriers was considered. A sampling rate of 100 KHz was used, since this is the sampling rate of the DAC. Were used 512 points for the discrete Fourier transform and 200 symbols for the window. Several simulations were performed for different guard intervals ranging from 0 to 16 samples. To simulate the channel was initially considered a model with 5-taps in the time domain and with an attenuation of 30 dB. The purpose of these simulations was to determine the appropriate guard interval for transmission.

The QAM and PSK modulations were tested to modulate each subcarrier. The frequency response of the channel was calculated to the signal sent and the frequency response of the channel was also estimated through the received signal. In order to have a better comparison tool between the different modulations, the bit/noise ratio (E_b/N_0) was calculated by the following equation expressed in dB:

$$\frac{E_b}{N_0} = SNR - 10log_{10}\left(\frac{R_b}{B}\right)$$

Where R_b represents the bitrate and B represents the bandwidth in Hz.

In order to try to obtain results with some precision, 200 transmissions were simulated for each modulation, for SNR values between 0 and 45 dB and for several values of multipath dispersion. We averaged the binary error rate of the 200 transmissions for each SNR value. As already said, we began by characterizing the 5-taps channel in the time domain. A 3-channel and 8-taps channel was also tried. These simulations were performed as previously reported for guard intervals 4, 8 and 16 samples. The value of BER with FEC was set at $3.8 * 10^{-3}$ and the value of the SNR needed to obtain an error rate smaller than this value was compared for each modulation.

As previously reported, tests were performed on 3, 5 and 8-channel channels in order to observe the consequence of more pathways in the binding. The values obtained did not differ enough to be significant. That is, in the 3-taps and 8-taps tests the results were always with a difference of less than 1dB of the tests performed with 5-taps.

V. Experimental Implementation

A. Objective

The experimental setup was based on the block diagram of Figure 6. The OFDM signal transmission in free space was divided into three blocks. The first one was to create the signal using a Matlab script according to the parameters chosen for this work (number of total subcarriers and data subcarriers,

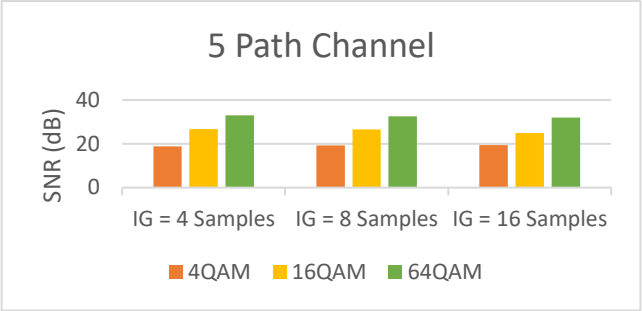

Fig. 6. Minimum SNR for 5 path channel using QAM and FEC

available bandwidth, cyclic prefix duration and QAM or PSK mapping level). In the second block, the signal was used to

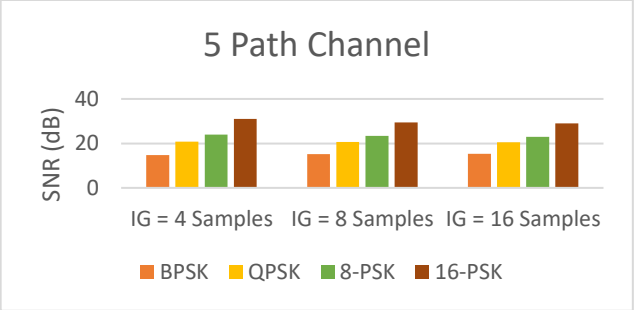

Fig. 7. Minimum SNR for 5 path channel using PSK and FEC

directly modulate the laser using a DAC, sending the signal through the atmospheric channel, being converted again to the electrical domain through the photodetector DET10A/M and passing through the DAC in order to convert the signal to digital. Finally the digital signal is sent to Matlab in order to be demodulated and the evaluation parameter BER is calculated. PSK and QAM modulations were tested to modulate the OFDM signal subcarriers.

In order to obtain a more reliable result, 8 tests were performed for each experiment in which the modulation index, the number of Fourier transform points, the number of subcarriers and the number of symbols sent were varied.

The first modulation used in order to test the system was the OOK modulation since it is a fairly simple modulation. For this first experiment the lens with the lowest optical density was used, in this case 0.5 which corresponds to a signal sent 3.16 times more powerful than the received signal. It was found that in order to receive the signal it was necessary to lower the intensity of the Laser. For this it was necessary to reduce the range of values sent from [0.5; 4.5] Volts for [0.1; 2.5] Volts. This method can be used without problem for this modulation since we are only using 1bit, i.e. to send the value 0 modulates the laser with 0.1V and to send the value 1 modulates with 2.5 V. This method becomes impossible to use for other more complex modulations since this modulations get to use in the worst case 6 bits which causes the signal to be quantized in 64 parts, leaving the quantization intervals too close together, making it impossible to detect with reasonable error values.

When using OFDM, the range of values sent to the Laser was again passed to [0.5; 4.5] Volts in order to obtain larger quantization intervals. The various lenses of the FW1AND filter holder were then used to test the maximum attenuation supported by each sub modulation. In optical

communications, BER values in the order of 10^{-12} are considered acceptable which reasonably gives an error in each trillion bits sent. There is a method for transforming a BER in the order of 10^{-3} into a BER capable of being used in an optical transmission system. This method has the name of Forward Error Correction (FEC). The value then set as the maximum limit of the rate of binary errors in the transmission was $3.8 * 10^{-3}$.

B. Results

As previously mentioned in order to evaluate and test the implemented system the OOK modulation was used in the first instance since it is the most basic, using only two voltages one for bit 1 and one for bit 0. In this first test of the system the lens with an optical density of 0.5 was used, which is equivalent to an attenuation of 5dB. The power of the signal sent by the laser is 38.2 dBm. In this test 40 bits were sent at a binary rate of 5 Kbit/s with a SNR of 21.97 dB, no error having been detected thus having a BER = 0. This modulation was, however, only used to test the system since it has a very low efficiency and the purpose of this dissertation was the implementation of OFDM.

As already mentioned, the modulated signal of OFDM, depending on the modulation index of the subcarriers, is divided into different quantization intervals. For example, in the case of BPSK we work with 2 quantization intervals. In the case of 4PSK or 4QAM we work with 4 intervals, 8PSK works with 8 intervals, 16PSK and 16QAM with 16 intervals and finally 64QAM implies 64 intervals of quantization. Working with these modulations prevents us from using the same method used in OOK modulation, since by decreasing the amplitude in the signal sent from [0.5; 4.5] V for [0.1; 2.5] V so as not to saturate the detector the quantization intervals are too close to each other so decoding in the receiver becomes impossible.

The alternative is to lower the power reaching the receiver, since the average power of the Laser is fixed at 38.2 dBm, it is necessary to use the filter station in order to attenuate the signal in the optical regime. The various lenses were tested. Between the optical density lens 0.5 and the lens with optical density 2.0 the laser intensity is too high. Then follow the tests performed with the optical density lens 2.0 which corresponds to an attenuation of 20 dB.

1) 20 dB Atenuation

In this experiment a signal with 1040 symbols was generated using 64 points in the Fourier transform and 20 subcarriers and was tested only once for each modulation of the subcarriers since the error values were exaggeratedly high. We started by testing the BPSK modulation having obtained a binary error rate of 0.257 with a SNR of 21.10dB. Then the QPSK modulation was tested with the same number of points of the Fourier transform, as well as the same number of subcarriers having been sent the number of symbols of the previous test. A binary error rate of 0.311 was obtained with a SNR of 21.09 dB. The 8PSK modulation was also tested with the same number of points of the Fourier transform, as well as the same number of subcarriers having been sent the number of symbols of the previous tests, obtaining a binary error rate of 0.424 with a SNR of 21.14 dB.

With respect to the PSK modulation of the subcarriers the 16PSK modulation with the same number of points of the Fourier transform was also tested, as well as the same number of subcarriers having been sent the number of symbols of the previous tests, obtaining a rate of binary errors of 0.454 with a SNR of 21.23 dB.

Once the various PSK modulation indices were tested to modulate the subcarriers, we proceeded to the use of QAM. The whole process was repeated using the same number of Fourier transform points as the same number of subcarriers having been sent the number of symbols from the previous tests. We started by testing 4QAM, obtaining a binary error rate of 0.282 with a SNR of 20.73 dB. The next step was to test the 16QAM modulation, obtaining a binary error rate of 0.384 with a SNR of 21.04 dB.

Finally, in the last test performed with this lens, using the same number of Fourier transform points and the same number of subcarriers, the subcarriers were modulated in 64QAM, obtaining a binary error rate of 0.42 with a SNR of 20.92 dB. It becomes easy to verify the attenuation of the lens 4 with an optical density of 2.0 equivalent to an attenuation of 20 dB is too low, which causes saturation in the receiver, making it impossible to correctly detect the emitted signal, since the laser intensity was too high. Thus, the lens 5 was tested which corresponds to an optical density of 3.0 which implies an attenuation of 30 dB in the optical signal domain.

2) 30 dB Atenuation

Eight tests were performed for each sub modulation, 4 during the day and 4 during the night in order to verify possible influences of the luminosity in the transmission. The BPSK modulation was tested first, and no errors were obtained in any of the tests. 44160 symbols were sent using 200 subcarriers, 512 points for the Fourier transform, and a binary rate of 31.4 Kbps was obtained as well as a SNR of 20.66 dB. The signal at the output of the transmitter is shown in blue and at the input of the receiver is represented in red,

FFT = 512		Subcarriers = 160				Symbols= 44160				Rb = 31.4Kbps		
DAY						NIGHT						
Test 1	Errors	0	Test 2	Errors	0	Test 1	Errors	0	Test 2	Errors	0	
	BER	<1/44160		BER	<1/44160		BER	<1/44160		BER	<1/44160	
Test 3	Errors	0	Test 4	Errors	0	Test 3	Errors	0	Test 4	Errors	0	
	BER	<1/44160		BER	<1/44160		BER	<1/44160		BER	<1/44160	
Average	Errors	0				Average	Errors	0				
	BER	<1/44160					BER	<1/44160				
Final Average	Errors	0										
	BER	<1/44160										

Fig. 8. Experimental results using BPSK

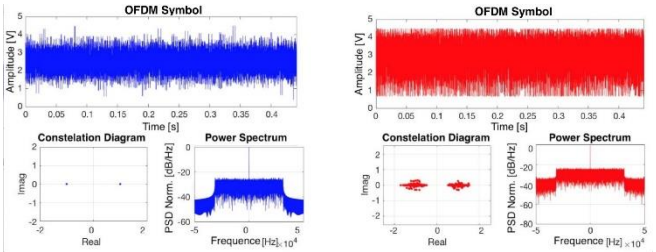

Fig. 9. Transmission using BPSK

Then the QPSK modeling was tested using the same number of Fourier transform points as the same number of subcarriers. The same 8 tests were done, and no error was obtained. The same number of symbols were sent, obtaining a binary rate of 62.7 Kbps with a SNR of 20.99 dB.

FFT = 512		Subcarriers = 160				Symbols= 44160				Rb = 62.7Kbps	
DAY						NIGHT					
Test 1	Errors	0	Test 2	Errors	0	Test 1	Errors	0	Test 2	Errors	0
	BER	<1/44160		BER	<1/44160		BER	<1/44160		BER	<1/44160
Test 3	Errors	0	Test 4	Errors	0	Test 3	Errors	0	Test 4	Errors	0
	BER	<1/44160		BER	<1/44160		BER	<1/44160		BER	<1/44160
Average	Errors	0				Average	Errors	0			
	BER	<1/44160					BER	<1/44160			
Final Average	Errors	0									
	BER	<1/44160									

Fig. 10. Experimental results using QPSK

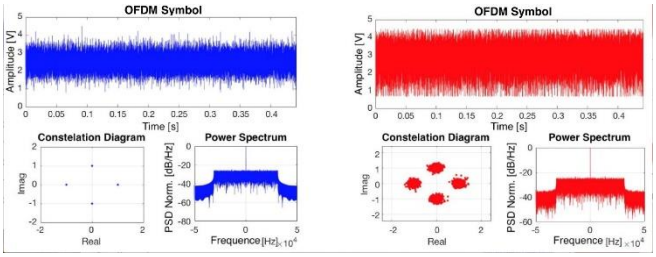

Fig. 11. Transmission using QPSK

We moved to the 8PSK modulation test and some errors were detected here. The test conditions were the same as in the previous tests. Having achieved a binary rate of 94.1 Kbps with a SNR of 21.24 dB.

FFT = 512		Subcarriers = 160				Symbols= 44160				Rb = 94.1Kbps	
DAY						NIGHT					
Test 1	Errors	11	Test 2	Errors	100	Test 1	Errors	89	Test 2	Errors	16
	BER	0.0003		BER	0.00271		BER	0.00241		BER	0.00043
Test 3	Errors	51	Test 4	Errors	37	Test 3	Errors	0	Test 4	Errors	22
	BER	0.0014		BER	0.001		BER	<1/44160		BER	0.0006
Average	Errors	49.75				Average	Errors	31.75			
	BER	1.35E-03					BER	8.60E-04			
Final Average	Erros	40.75									
	BER	1.11E-03									

Fig. 12. Experimental results using 8PSK

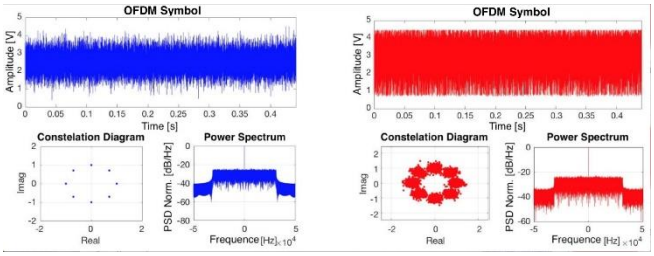

Fig. 13. Transmission using 8PSK

Finally, the 16PSK modulation test was performed where errors were also detected and recorded in Table 9. The test conditions were the same, a binary rate of 125.5 Kbps with a SNR of 21.24 dB was obtained. Figure 61 shows the transmission of the signal.

FFT = 512		Subcarriers = 160				Symbols= 44160				Rb = 125.5Kbps	
DAY						NIGHT					
Test 1	Errors	2377	Test 2	Erros	2783	Test 1	Errors	2002	Test 2	Errors	2419
	BER	0.04823		BER	0.05647		BER	0.04063		BER	0.04909
Test 3	Errors	3176	Test 4	Erros	2743	Test 3	Errors	1415	Test 4	Errors	1756
	BER	0.06445		BER	0.0556		BER	0.029		BER	0.03564
Average	Errors	2769.75				Média	Errors	1898			
	BER	5.62E-02					BER	3.86E-02			
Final Average	Errors	2333.875									
	BER	4.74E-02									

Fig. 14. Experimental results using 16PSK

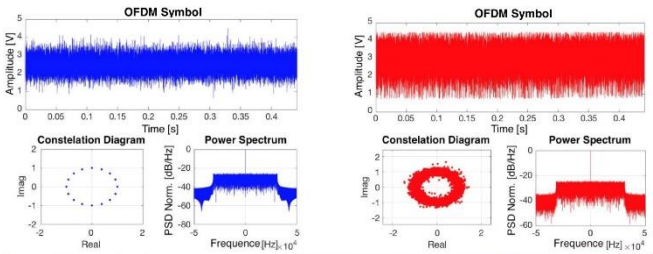

Fig. 15. Transmission using 16PSK

Once the various PSK modulation indices for the subcarriers were tested, it was then switched to QAM modulation. The first one to be tested was 4QAM, using the same parameters of the previous tests. Table 10 represents the various tests performed, obtaining a binary rate of 62.7 Kbps with a SNR of 20.70 dB.

FFT = 512		Subcarriers = 160				Symbols= 44160				Rb = 62.7Kbps	
DAY						NIGHT					
Test 1	Errors	0	Test 2	Errors	0	Test 1	Errors	0	Test 2	Errors	0
	BER	<1/44160		BER	<1/44160		BER	<1/44160		BER	<1/44160
Test 3	Errors	0	Test 4	Errors	0	Test 3	Errors	0	Test 4	Errors	0
	BER	<1/44160		BER	<1/44160		BER	<1/44160		BER	<1/44160
Average	Errors	0				Average	Errors	0			
	BER	<1/44160					BER	<1/44160			
Final Average	Errors	0									
	BER	<1/44160									

Fig. 16. Experimental results using 4QAM

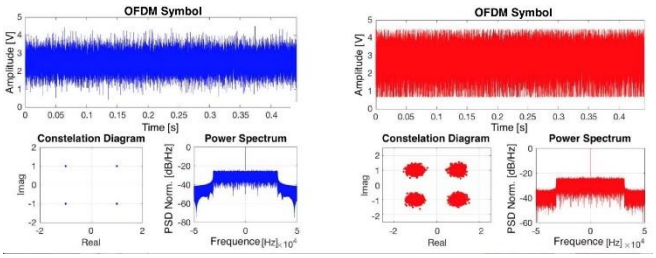

Fig. 17. Transmission using 4QAM

Once the 4QAM tests were performed, the modulation index was increased to 16QAM, maintaining the same parameters of the previous tests. Table 11 represents the various tests performed, obtaining a binary rate of 125.5 Kbps with a SNR of 20.70 dB.

FFT = 512		Subcarriers = 160				Symbols= 44160				Rb = 125.5Kbps	
DAY						NIGHT					
Test 1	Errors	390	Test 2	Errors	589	Test 1	Errors	142	Test 2	Errors	653
	BER	0.00791		BER	0.01195		BER	0.0029		BER	0.01325
Test 3	Errors	136	Test 4	Errors	749	Test 3	Errors	331	Test 4	Errors	369
	BER	0.00276		BER	0.015		BER	0.0067		BER	0.00749
Average	Errors	466				Average	Errors	373.75			
	BER	9.41E-03					BER	7.58E-03			
Final Average	Errors	419.875									
	BER	8.50E-03									

Fig. 18. Experimental results using 16QAM

Finally, 64QAM tests were performed, maintaining the parameters of the previous tests.

FFT = 512		Subcarriers = 160				Symbols= 44160				Rb = 188.2Kbps	
DAY						NIGHT					
Test 1	Errors	6179	Test 2	Errors	7493	Test 1	Errors	6140	Test 2	Errors	4474
	BER	0.08359		BER	0.10137		BER	0.08306		BER	0.06052
Test 3	Errors	3919	Test 4	Errors	7417	Test 3	Errors	5152	Test 4	Errors	4362
	BER	0.053		BER	0.1		BER	0.0697		BER	0.059
Average	Errors	6252				Average	Errors	5032			
	BER	8.45E-02					BER	6.81E-02			
Final Average	Erros	5642									
	BER	7.63E-02									

Fig. 19. Experimental results using 64QAM

Since no errors were detected in the use of BPSK, QPSK and 4QAM with lens 5 corresponding to an optical density of 3.0 equivalent to an attenuation of 30 dB, the optical density of the lens was increased in order to calculate the maximum of attenuation supported by these modulations. It was then passed to the lens 6 having an optical density of 4.0 corresponding to an attenuation of 40dB.

3) 40 dB Atenuation

We started by testing BPSK modulation with the same number of symbols using the same number of subcarriers and the same number of points of the Fourier transform. Having

obtained a BER of $2.8 * 10^{-3}$ with a bit rate equal to 31.4 Kbps. Then the QPSK modulation was tested, obtaining a BER of $5.3 * 10^{-3}$ with a bit rate equal to 62.7 Kbps. Finally, the 4QAM modulation was tested, obtaining a BER of $3.75 * 10^{-3}$ with a bit rate equal to 62.7 Kbps.

VI. Conclusions

The guard intervals of 4, 8 and 16 samples were tested and the guard interval of 16 samples proved to be most suitable for modulation indices greater than 4.

Since the laser had a maximum power of 300 mw we were unable to pass from the 22 dB of SNR in the laboratory implementation, this was sufficient to achieve positive results for some modulations that require a lower SNR to achieve the binary error rate of $3.8 * 10^{-3}$ after the implementation of FEC. Other modulations with higher indices would require a higher power laser in order to meet the error rate requirements.

With respect to the 4QAM sub modulation, we can observe that in the simulations to obtain a lower BER for the transmission of the OFDM signal the average SNR is 19 dB, so it would be expected that we could transmit the signal within the limits of errors imposed for the transmission, since the SNR reached in the experimental implementation is 20.7 dB. The same is true since a BER value of 0 was obtained and no error was detected. Regarding the 16QAM sub modulation the SNR values of the channel simulation obtained for the desired maximum error rate was 25 dB. Since the SNR of the transmission was about 21 dB in the experimental implementation it was not possible to transmit using this sub modulation. The same happens for the 64QAM sub modulation, through the simulated channel a minimum SNR of 32 dB was obtained. Regarding the PSK sub modulation for an attenuation of 30 dB we only achieved positive results for BPSK QPSK and 8-PSK. The simulated mean SNR values for BPSK and QPSK were 15.3 dB and 20.5 dB respectively falling below the experientially obtained SNR. For 8-PSK it was obtained through the simulation of the transmission channel using the Matlab a SNR of 23 dB, nevertheless experimentally it was possible to obtain positive results using this modulation. This difference of about 1dB may be due to several error factors of both the simulated transmission component and the experimental component. For 16-PSK, the SNR obtained through simulation was 29 dB, and it was not possible to obtain positive results experimentally.

The most suitable modulation is the one that allows a higher bitrate by keeping the BER below the value set with FEC. Following these requirements, the 8PSK sub modulation with a binary rate of 94.1 Kbps and a BER of $1.1 * 10^{-3}$ is ideal for a 30 dB attenuation. Only the BPSK and 4QAM sub modulations were below the desired BER value for a 40 dB attenuation. Since with 4QAM a binary rate of two times greater than BPSK is obtained, this would be the ideal sub modulation for transmission with a binary rate of 62.7 Kbps and a BER of $3.75 * 10^{-3}$. Experiments were performed during the day and at night in order to measure the impact of the luminosity on the detector and a mean was made between daytime and night values in order to obtain more reliable results.

Higher transmission rates were also obtained if a DAC with a higher sampling rate had been used. With the continued evolution of the new devices there are now DACs with capacities of 10 Gsps, the use of one of these devices would raise the transmission rates of the house from Kbps to Gbps.

VII. References

[1] M. Uysal and H. Nouri, "Optical wireless communications — An emerging technology," *2014 16th Int. Conf. Transparent Opt. Networks*, pp. 1–7, 2014.

[2] Ericsson, "Mobility Report," *White Pap.*, no. May, pp. 7–8, 2016.

[3] Z. Ghassemlooy, S. Arnon, M. Uysal, Z. Xu, and J. Cheng, "Emerging Optical Wireless Communications-Advances and Challenges," *IEEE J. Sel. Areas Commun.*, vol. 33, no. 9, pp. 1738–1749, 2015.

[4] M. Uysal, C. Capsoni, and Z. Ghassemlooy, *Optical Wireless Communications - An Emerging Technology*. Springer, 2015.

[5] W. P. and S. R. Z. Ghassemlooy, *Optical Wireless Communications System and Channel Modelling with MATLAB*. CRC Press - Taylor & Francis Group, 2017.

[6] C. Kachris and K. Bergman, *Optical Interconnects for Future Data Center Networks*. Springer, 2013.

[7] I. Stefan, H. Burchardt, and H. Haas, "Area spectral efficiency performance comparison between VLC and RF femtocell networks," *IEEE Int. Conf. Commun.*, pp. 3825–3829, 2013.

[8] D. Tsonev *et al.*, "A 3-Gb/s single-LED OFDM-based wireless VLC link using a gallium nitride μLED," *IEEE Photonics Technol. Lett.*, vol. 26, no. 7, pp. 637–640, 2014.

[9] S. Yu, O. Shih, and H. Tsai, "Smart Automotive Lighting for Vehicle Safety," *IEEE Commun. Mag.*, no. December, pp. 50–59, 2013.

[10] G. Parca, A. Shahpari, V. Carrozzo, G. M. T. Beleffi, and A. L. J. Teixeira, "Optical wireless transmission at 1.6-Tbit/s (16×100 Gbit/s) for next-generation convergent urban infrastructures," *Opt. Eng.*, vol. 52, no. 11, p. 116102, 2013.

[11] H. Haan, M. Gerken, and M. Tausendfreund, "Long-range laser communication terminals: Technically interesting, commercially incalculable," *Proc. 2012 8th Int. Symp. Commun. Syst. Networks Digit. Signal Process. CSNDSP 2012*, pp. 3–6, 2012.

[12] T. Tolker-Nielsen and G. Oppenhauser, "In-orbit test result of an operational optical intersatellite link between ARTEMIS and SPOT4, SILEX," *Proc. SPIE 4635, Free. Laser Commun. Technol. XIV*, vol. 4635, pp. 1–15, 2002.

[13] H. Willebrand and B. S. Ghuman, "Free space optics: enabling optical connectivity in today's networks," p. 259, 2002.

[14] P. Kress, Bernard C.; Meyrueis, *Applied Digital Optics*. Chippenham, Wiltshire: John Wiley & Sons, Ltd Registered, 2009.

[15] S. D. Dissanayake and J. Armstrong, "Comparison of ACO-OFDM, DCO-OFDM and ADO-OFDM in IM/DD systems," *J. Light. Technol.*, vol. 31, no. 7, pp. 1063–1072, 2013.

[16] J. Armstrong, "OFDM for Optical Communications," *J. Light. Technol.*, vol. 27, no. 3, p. 16, 2009.

[17] Ka. Asadzadeh and B. S. Kasra Asadzadeh, "Efficient OFDM Signaling Schemes For Visible Light Communication Systems," p. 99, 2011.